The Phototoxic Effect of Gold-antibody-based Nanocarrier of Phthalocyanine on Melanoma Monolayers and Tumour spheroids

Nkune Williams Nkune and Heidi Abrahamse*

Supporting information

1. Characterization of Nanobioconjugate

1.1. UV–Visible Spectroscopy Analysis

Jenway Genova Nano Plus Life Science Spectrophotometer (Cole-Parmer Ltd., Stone, Staffordshire, UK) was used verify the distinctive optical features of the NBC and its components. The samples were pipetted into optical quartz cuvette and measured for absorbance from 200 to 800 nm wavelengths. 0.001 M PBS was used as the standard. Increasing concentrations of free $ZnPcS_4$ (10-60 µM) were spectrophotometrically measured at 673 nm, and a standard curve was plotted to estimate the amount of the PS bound to $ZnPcS_4$-AuNP-S-PEG-NH_2-anti-MIA Ab and the loading capacity. The following equations were derived from the standard curves of $ZnPcS_4$ (Y = 0.0013x + 0.0017), AuNPs (Y = 0.0006x - 0.0131) and Anti-MIA Ab (Y = 0.0155x + 0.0235) and loading capacity was determined using the following formula:

$$\text{loading capacity } \% = \frac{concetration\ of\ loaded\ PS}{concentration\ of\ PS\ in\ feed} \times 100.$$

1.2 Dynamic Light Scattering (DLS) and Zeta Potential

The NBC and single components' sizes and zeta potentials were determined by the DLS technique provided by Zetasizer Nano ZS (Malvern Instruments, Malvern, UK). The sonicated samples were diluted with deionized water, and the contents were vortexed for a few minutes. The analysis was conducted at 25°C using 13° and 173° scattering angles. The Malvern software was used to calculate the Z-average diameter as well as the zeta potential to determine the surface charge based on electrophoretic mobility.

1.3 Morphological and Size Analysis

The size and morphology of the NBC were acquired using JEM-2100 High Resolution Transmission Electron Microscope (HR-TEM) (JEOL Ltd.). The homogenized prepared samples were dripped on the carbon coated copper grids. ImageJ v1.53 software (National Institutes of Health and Laboratory for Optical and Computational Instrumentation (LOCI), University of Wisconsin, United States of America) was utilized to measure the diameter of the NBC. Energy-dispersive X-ray spectroscopy (EDX) device attached to TEM was used to analyse elements within the samples.

1.4 Fourier Transform Infrared (FTIR) Analysis

FTIR was employed to confirm the chemical interactions between $ZnPcS_4$, PEGylated AuNPs, and Anti-MIA Ab. The samples were freeze-dried for 3 days and ground into a powder. The pellets of the prepared samples were formed by dispersing them in a KBr matrix and subjecting the mixture to compression at high pressure. Absorbance spectra were carried out at with 25 scans using The FTIR (Perkin Elmer Spectrum 100 FTIR spectrometer, University of Johannesburg, Analytical Chemistry Department) from 400 to 4000 cm^{-1} wavenumbers.

1.5 loading Capacity

2. Results

2.1 UV-Vis spectral analysis

2.1.1 Optical characteristics of single molecules

The UV-Vis spectroscopy screened the single molecules for their intrinsic optical hallmarks before they underwent chemical reactions. As shown in Figure S1A, the UV-Vis spectra of $ZnPcS_4$ displayed its typical peaks (340, 634, and 673 nm). The 673 nm peak has garnered attention in PDT explorations. AuNPs' spectra gave an anticipated peak at 520 nm (Figure S1B). Studies have highlighted that antibodies' peaks normally appear within the 250-280 nm region, which coincides with the Anti-MIA Ab spectra (260 nm) in Figure S1C[1]. The absorption spectra of the NBC ($ZnPcS_4$-AuNP-Ab) displayed all the characteristic peaks of its components (Figure S1D). However, notable broadening and AuNP resonance peak shifting (533 nm) were observed, which indicated definite chemical interactions between $ZnPcS_4$, AuNP, and anti-MIA Ab[2].

Laser Research Centre, Faculty of Health Sciences, University of Johannesburg, P.O. Box 17011, Doornfontein 2028, South Africa; 217078898@student.uj.ac.za*Correspondence: habrahamse@uj.ac.za; Tel.: +27-11-559-655

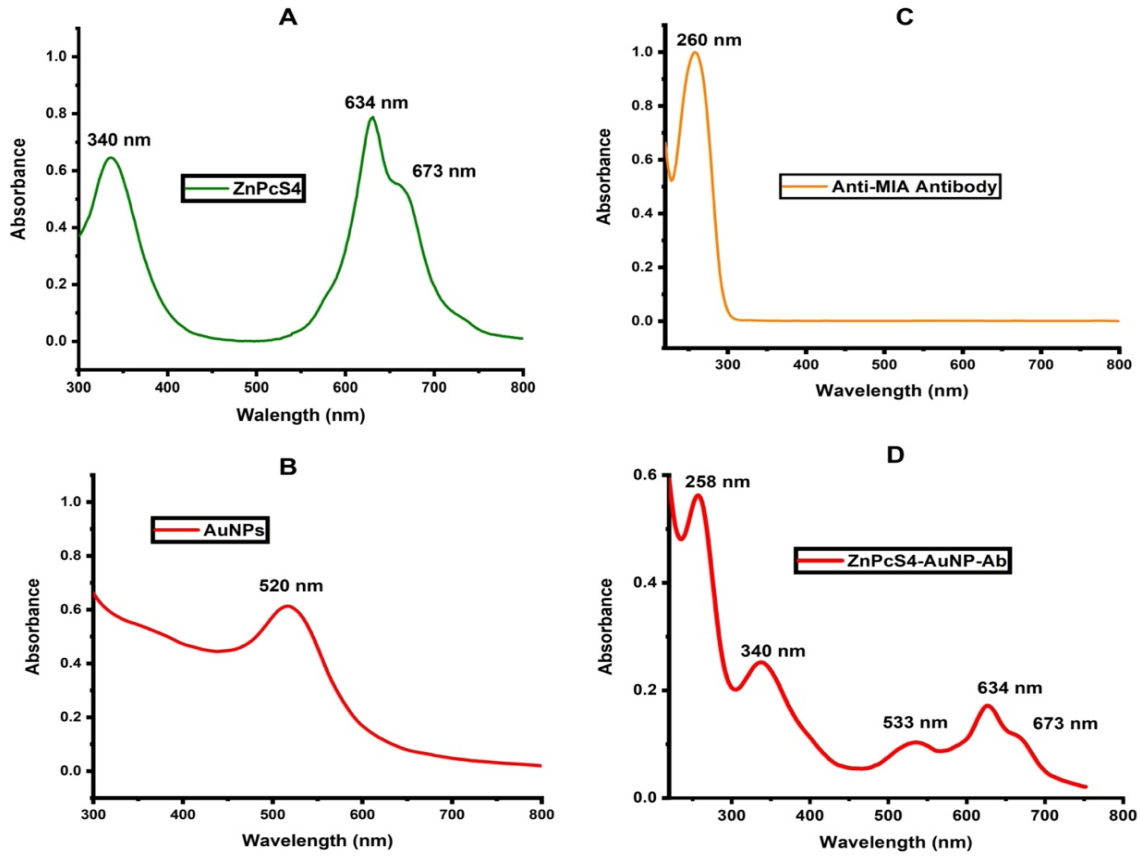

Figure S1. The UV-visible of spectral analysis. **(A)** $ZnPcS_4$ **(B)** PEGylated AuNP **(C)** Anti-MIA and **(D)** Nanobioconjugate ($ZnPcS_4$-AuNP-Anti-MIA).

2.1.2 FTIR

The FTIR spectra of $ZnPcS_4$ and $ZnPcS_4$-AuNP have been reported in our previous study [3]. As illustrated in Figure S2, 1700 cm^{-1} within the anti-MIA Ab FTIR spectrum correlated to the C=O function group, whereas 1638–1607 absorption peaks represented the N–H of the antibody. Further analysis demonstrated that the NBC ($ZnPcS_4$-AuNP-Ab) spectra closely resembled the distinct peaks of $ZnPcS_4$ and AuNP. On that note, the 1096 cm^{-1} peak corresponded to the C-O-C functional group of the PEG bound to AuNP. Furthermore, S=O stretching from sulfonate groups of $ZnPcS_4$ was noted at 1379 cm^{-1}, suggesting the presence of the PS in the NBC[4]. Lastly, the amide bond between the AuNP and the Ab was confirmed by the presence of the N-H bending at 1610–1560 cm^{-1} [5].

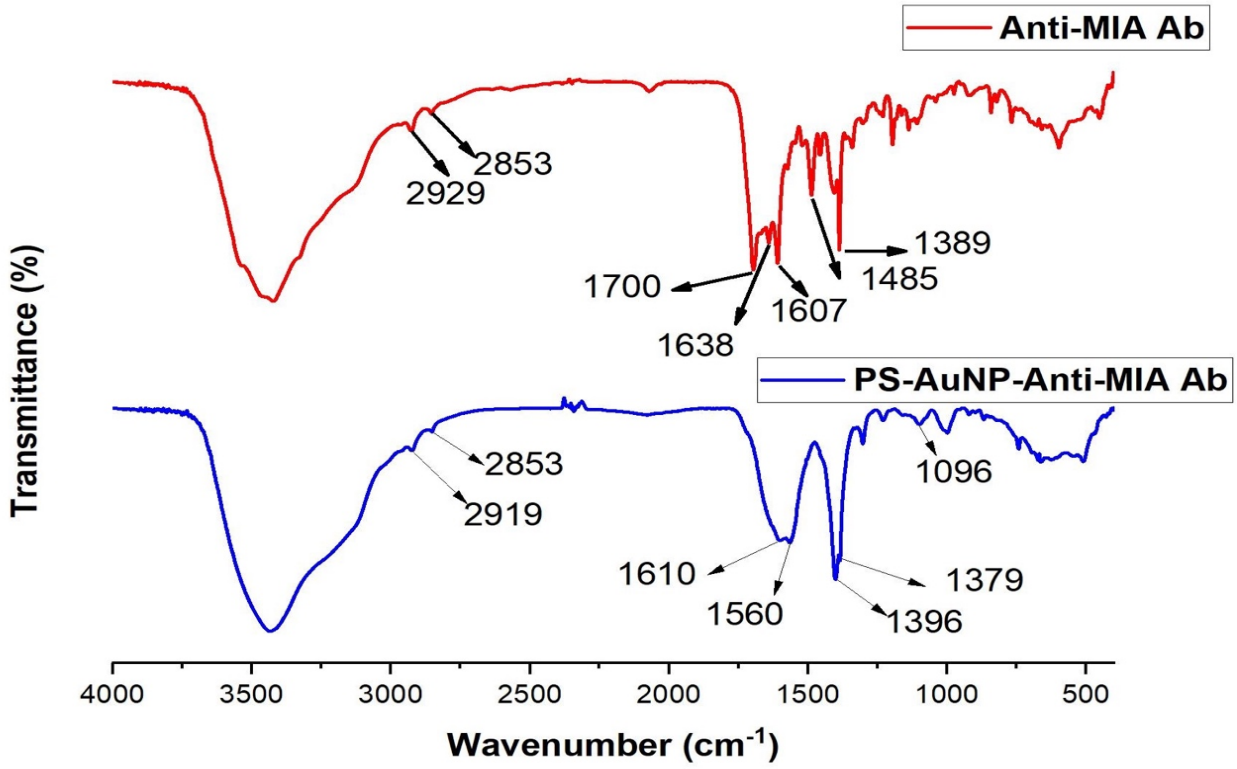

Figure S2. The FTIR analysis of the NBC confirming the successful bonding of the Anti-MIA onto the surface of $ZnPcS_4$-AuNP.

2.1.3 Particle size and surface charge of the nanobioconjugate

The hydrodynamic diameter and Zeta potential of the NBC were found to be 215.6 nm and -19.1 mV, respectively. This hydrodynamic diameter is greater than that of AuNPs (44.57 nm), $ZnPcS_4$ (53.12 nm), and $ZnPcS_4$-AuNP (61.68 nm), which we previously reported. This notable increase in size is indicative of definitive chemical reactions between the components, resulting in an increase in molecular weight. The negative electrostatic charge of the NBC clearly suggests its stability in an aqueous condition, which is attributed to PEGylation[6]. Furthermore, the NBC exhibited a PDI value of 0.353, indicative of a remarkable distribution and no apparent aggregation. When compared to the AuNPs TEM results from our previous study[3], the NBC was spherical with an average size of about 14 nm, showing no morphological changes or agglomeration (Figure S3A) DLS tends to exhibit bigger sizes than TEM due to its preference for larger particles [7]. Additionally, EDS analysis revealed that the NBC contained carbon (C), oxygen (O), zinc (Zn), and gold (Au) elements (Figure S3B). However, the detected Cu atoms pertained to the Cu elements of the grid used for EDS analysis.

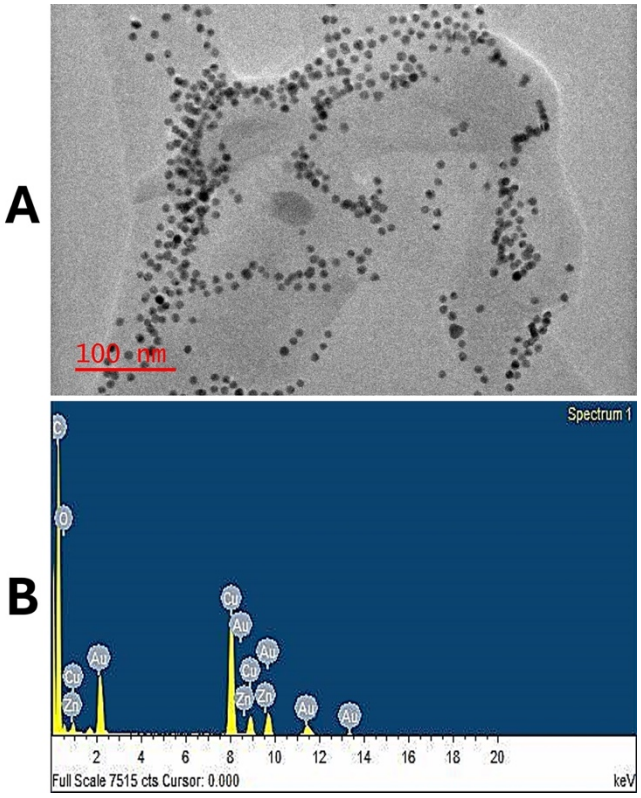

Figure S3. (A) TEM micrographs of NBC showing the presence of Anti-MIA Ab (B) EDS spectral analysis of the NBC.

2.1.4 Photostability

UV-Vis spectroscopy was once again used to detect the absorption peaks of the NBC over the course of five weeks for stability check. As illustrated in Figure S4, the ant-MIA Ab peak (258 nm) was detected within the NBC spectra, suggesting that the PS maintained its targeting abilities. Similarly, an important peak for PDT applications, 674 nm remained intact. These findings suggested that the $ZnPcS_4$ within the NBC spectra retained its photodynamic properties with no apparent photobleaching. In addition, the AuNP SPR peak (533 nm) also remained prominent with no sign of agglomeration, suggesting excellent cellular uptake in A375 spheroids.

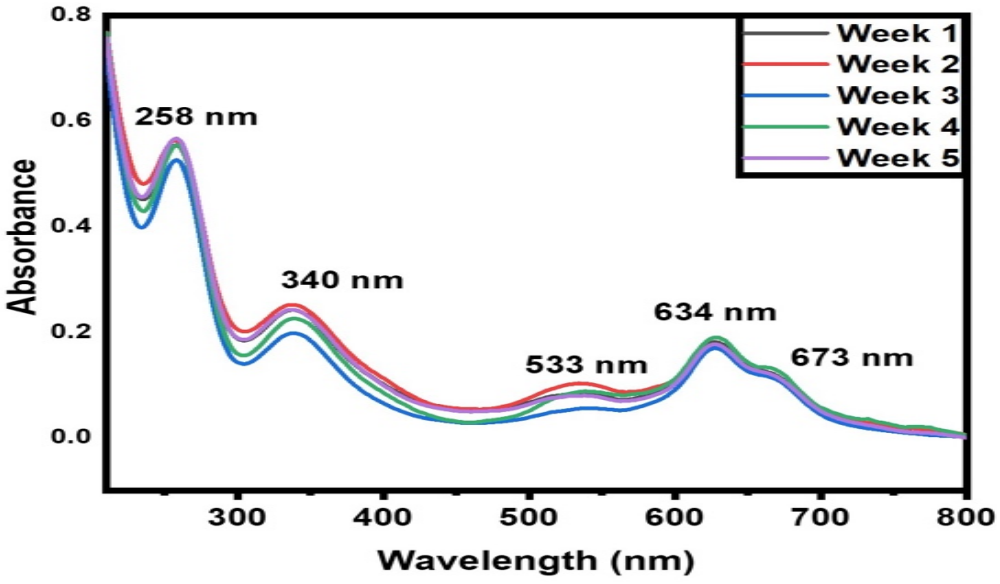

Figure S4. UV-vis spectral analysis of the NBC. **Anti-MIA Ab Peak** (258 nm), **$ZnPcS_4$ peaks (**340 nm, 634 and 673 nm) and **AuNP peak** (533 nm).

2.1.5 Loading Capacity

Table S1 shows estimated concentrations of $ZnPcS_4$, AuNPs, and anti-MIA Ab bound to the NBC, which were calculated using equations derived from their standard concentration curves. The bound amount of $ZnPcS_4$ was 76 µM, AuNPs was 122 µg/mL and anti-MIA Ab was 35 µg/mL, whereas the loading capacity was found to be 60.8%.

Table S1 Estimated amounts of $ZnPcS_4$, AuNPs, and Anti-MIA Ab bound to the NBC

Sample	**Amount of $ZnPcS_4$ (absorbance = 0.10)**	**Amount of AuNPs (absorbance = 0.06)**	**Amount of anti-MIA Ab (absorbance = 0.56)**
NBC	76 µM	122 µg/mL	35 µg/mL

References

1 S. Prasad, I. Mandal, S. Singh, A. Paul, B. Mandal, R. Venkatramani and R. Swaminathan, Near UV-Visible electronic absorption originating from charged amino acids in a monomeric protein, *Chem. Sci.*, 2017, **8**, 5416–5433.

2 A. Crous and H. Abrahamse, Effective Gold Nanoparticle-Antibody-Mediated Drug Delivery for Photodynamic Therapy of Lung Cancer Stem Cells, *Int J Mol Sci*, , DOI:10.3390/ijms21113742.

3 N. Nkune and H. Abrahamse, The Efficacy of Zinc Phthalocyanine Nanoconjugate on Melanoma Cells Grown as Three-Dimensional Multicellular Tumour Spheroids, *Pharmaceutics*, 2023, **15**, 2264.

4 H. Montaseri, N. Nkune and H. Abrahamse, Active Targeted Photodynamic Therapeutic Effect of Silver-based Nanohybrids on Melanoma Cancer Cells, *Journal of Photochemistry and Photobiology*, 2022, **11**, 100136.

5 Y. Ji, X. Yang, Z. Ji, L. Zhu, N. Ma, D. Chen, X. Jia, J. Tang and Y. Cao, DFT-Calculated IR Spectrum Amide I, II, and III Band Contributions of N-Methylacetamide Fine Components, *ACS Omega*, 2020, **5**, 8572–8578.

6 R. Stiufiuc, C. Iacovita, R. Nicoara, G. Stiufiuc, A. Florea, M. Achim and C. M. Lucaciu, One-Step Synthesis of PEGylated Gold Nanoparticles with Tunable Surface Charge, *Journal of Nanomaterials*, 2013, **2013**, e146031.

7 N. Simelane, G. Matlou and H. Abrahamse, Photodynamic Therapy of Aluminum Phthalocyanine Tetra Sodium 2-Mercaptoacetate Linked to PEGylated Copper–Gold Bimetallic Nanoparticles on Colon Cancer Cells, *International Journal of Molecular Sciences*, 2023, **24**, 1902.